Soft Matter

ARTICLE TYPE

Cite this: DOI: 00.0000/xxxxxxxxxx

Supporting Information: Poroelasticity and permeability of fibrous polymer networks under compression

Paul Mollenkopf,[a] Jakub A. Kochanowski,[a] Yifei Ren,[b] Kyle H. Vining, [c] Paul A. Janmey, [a] and Prashant K. Purohit[b]

1 Flux

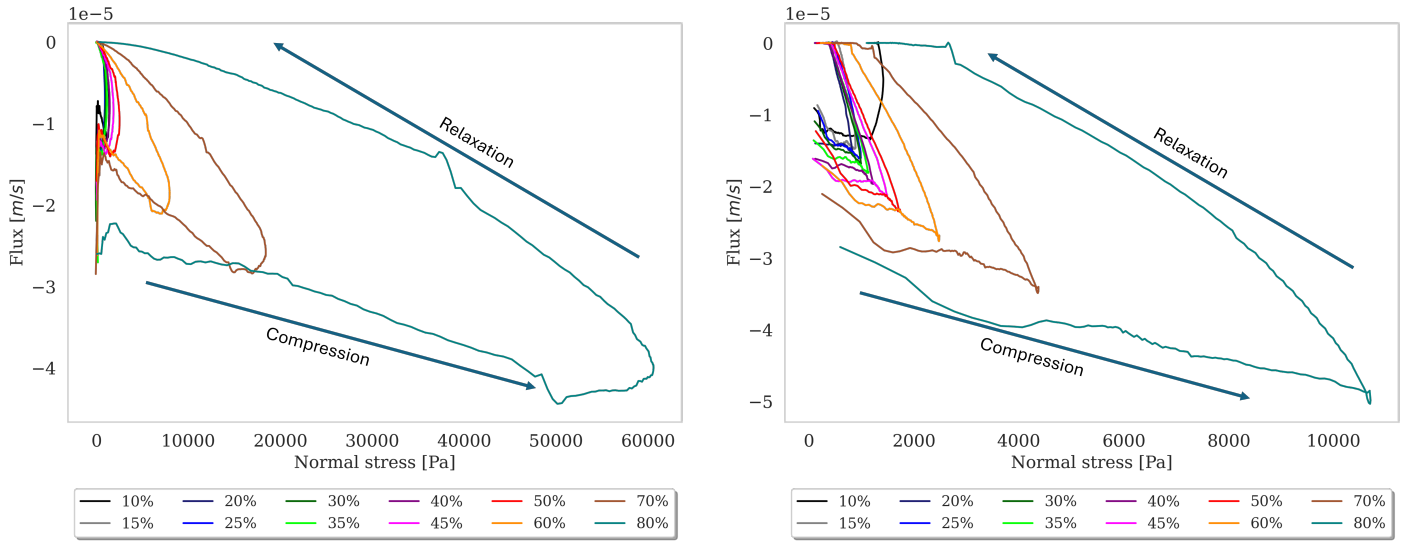

(a) Fibrin: Flux over normal stress.

(b) Collagen: Flux over normal stress.

Fig. 1 Flux over normal stress for fibrin (left) and collagen (right). The plots show the flux values for the compression as well as for the relaxation phase as indicated by the arrows. For the calculation of the Darcy permeability by fitting the curves to a linear function, the last part of the relaxation part of each curve was used (see Fig. 3 a,b in the main manuscript).

[a] *Department of Physiology, University of Pennsylvania, Philadelphia, PA, 19104 USA*
[b] *Department of Mechanical Engineering and Applied Mechanics, University of Pennsylvania, Philadelphia, PA 19104, USA*
[b] *Department of Preventive and Restorative Sciences, Department of Materials Science and Engineering, University of Pennsylvania, Philadelphia, PA 19104, USA*

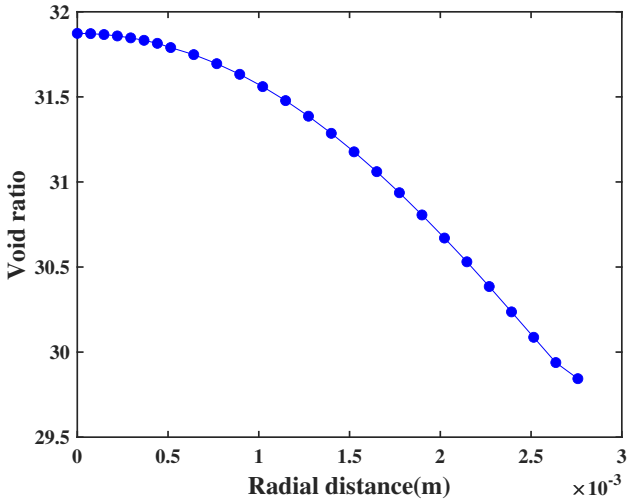

Fig. 2 A non-uniform void ratio along radial direction right before relaxation finishes. The non-uniform void ratio is coupled to a pore pressure (or chemical potential) gradient in the radial direction.

2 Permeability versus protein concentration

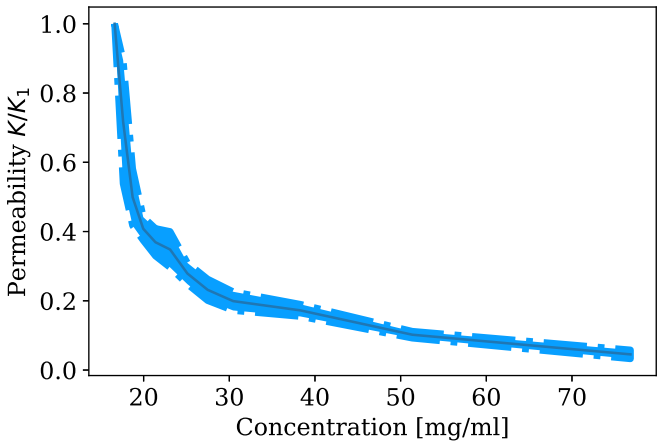

(a) Fibrin: Darcy permeability versus absolute protein concentration.

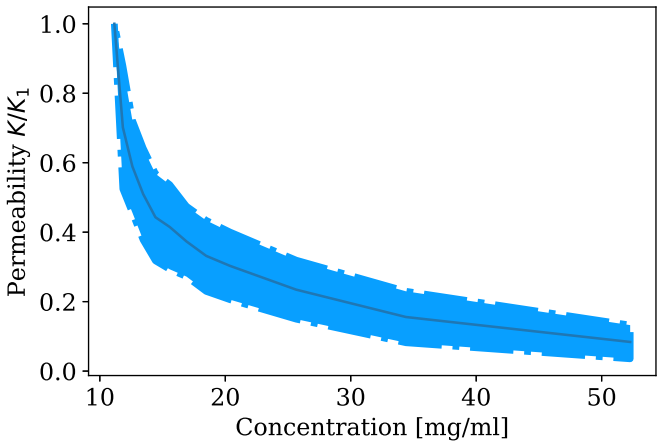

(b) Collagen: Darcy permeability versus absolute protein concentration.

Fig. 3 Darcy permeability over absolute protein concentration for fibrin (a) and collagen (b). Average Darcy constants are plotted over protein concentrations, calculated from the gels' initial concentrations and the fluid volume leaked from the gel sample during and after each compression step.

3 Microscope compression device

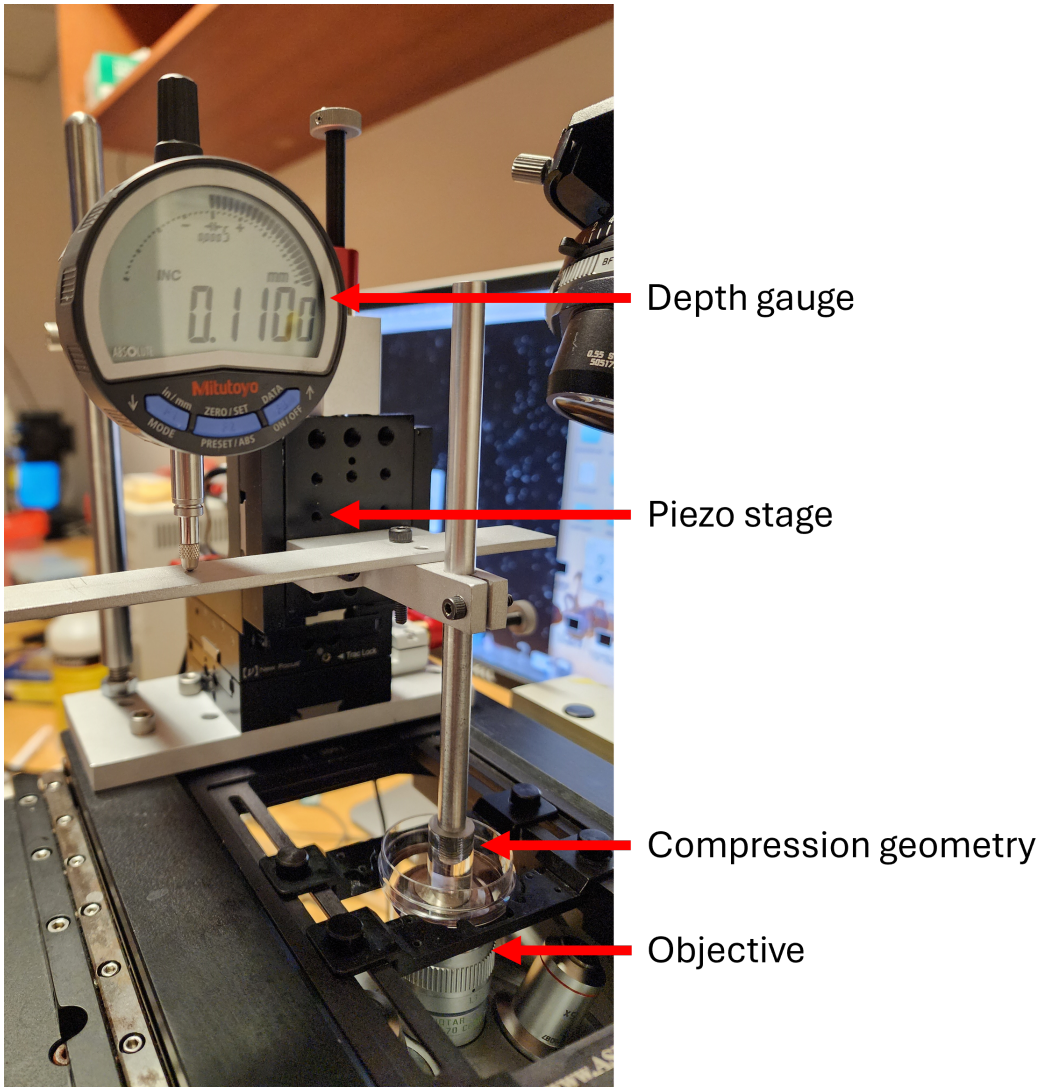

Fig. 4 Compression device: The setup consists of a three axis linear stage, each controlled by a piezoelectric motor (Newport model 9064-XYZ-PPP-M). The motors are connected to an open-loop controller that allows for interfacing with a computer, not imaged (Newport model 8742-4-KIT). The stage is attached to a custom-made aluminum adapter plate that attaches the setup to the microscope stage. To this plate is also attached a pole that holds a digital indicator (Mitutoyo item number 543-701). The indicator is connected to a computer using a USB Input Tool Direct cable, not imaged (Mitutoyo item number 06AGQ001F). To the plate of the three axis stage is attached a custom-machined geometry that holds the top plate as well as a metal extrusion that allows the indicator to keep track of the relative position of the z-axis of the stage. In this way, using custom-written software, we create a closed-loop system which allows us to move the z-axis of our stage by a known, controlled, distance and velocity with theoretical maximum resolution of 0.5 microns. The hydrogel is polymerized in situ or approximately measured using a caliper and placed on a glass bottom dish to allow for imaging on a confocal microscope.

4 Densification

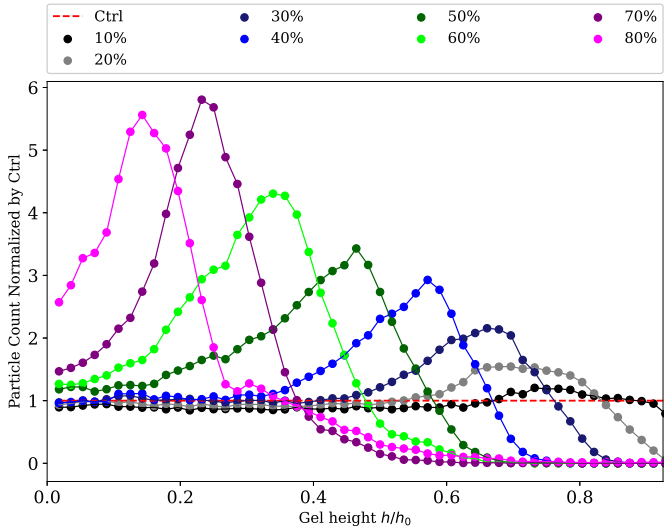

(a) Fibrin: Densification upon compression.

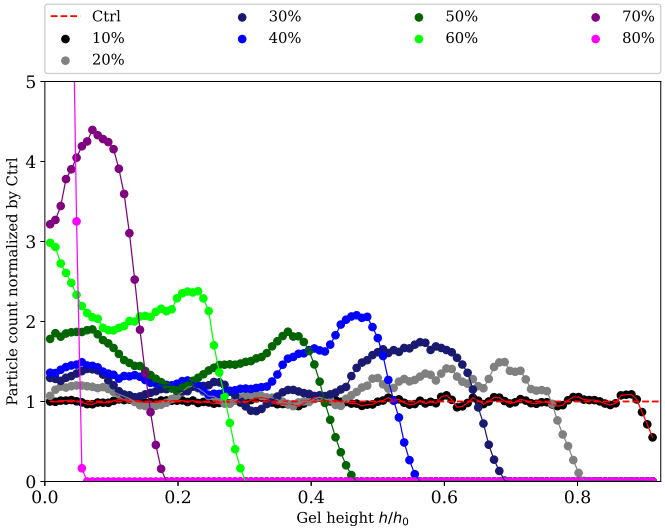

(b) Collagen: Densification upon compression.

Fig. 5 Gel densification after compressive strain steps. Counted particles, inserted into a gel by copolymerization, in vertical layers via z-stack imaging, reveal a non-uniform densification of fibrin and collagen gels upon successive compressions. The respective curves are divided by the control measurement, taken after polymerization and in an uncompressed state. Compressive strains, applied at a strain rate of 10μm/s, result in a gel densification in the upper layers of the gel, indicated by increased particle densities at the respective upper part of the gel, while the lower layers, where the curves do not deviate from the control measurement, stay unaffected. This is an alternative data representation for Fig. 6 in the main manuscript.